ELSEVIER

Contents lists available at ScienceDirect

Chemical Physics Letters

journal homepage: www.elsevier.com/locate/cplett





A first-principle investigate about the different response of birefringence and SHG from AB_3O_6 (A = Bi, Sb) compounds

Xuerui Shi ^{a,b,e}, Qun Jing ^{a,b,*}, Ming-Hsien Lee ^c, Haibin Cao ^d, Mengqiu Long ^{b,e,*}

- ^a Xinjiang Key Laboratory of Solid State Physics and Devices, Xinjiang University, Urumqi 830046, China
- b Institute of Low-dimensional Quantum Materials and Devices, School of Physical Science and Technology, Xinjiang University, Urumqi 830046, China
- ^c Department of Physics, Tamkang University, New Taipei City 25137, Taiwan
- ^d Department of Physics, College of Sciences, Shihezi University, Shihezi, 832000, China
- e Hunan Key Laboratory of Super Micro-structure and Ultrafast Process, Central South University, Changsha 410083, China

ABSTRACT

In this work, the electronic structures and optical properties of AB_3O_6 (A = Bi, Sb) are examined conducting the first-principles method at crystal and molecular level. The results show that the anionic groups and cation-centered polyhedra exhibit excellent optical properties due to their strong covalent bonds and optical anisotropy. The SbO and BiO groups own different responses of polarization anisotropy and first hyperpolarizability, resulting in different optical properties. Moreover, the states nearby the Fermi level of SBBO give positive and negative contribution to birefringence and SHG, which make it own stronger birefringence and smaller SHG comparison with BIBO.

1. Introduction

Nonlinear optical (NLO) materials have attracted widespread attention due to its application in the field of all-solid-state lasers, which can extend the output frequency of common laser sources [1–3]. To achieve excellent optical properties, researchers strive to achieve more [4–8], there are two aspects for nonlinear optical materials, the anionic groups with planar π conjugation were considered as priority candidates, including BO₃, CO₃ and NO₃ groups. Among them, BO group has attracted much attention because of its large polarizability, and a bunch of excellent compounds have been found based on BO group unit [9–17], classic materials include LiB₃O₅ (LBO)[18], CsB₃O₅(CBO) [19] and KBe₂BO₃F₂(KBBF) [20,21]etc.

Besides, introducing cation with lone pair electron was also a good strategy, because its stereochemical activity can lead to distorted crystal structures and excellent optical response [22,23]. Numerous outstanding compounds have been obtained under this strategy, such as BiB_3O_6 (BIBO) [24,25], $CsSbF_2SO_4$ [26], $MB_2O_3F_2$ (M=Sn, Pb) [27] and so on. Among these compounds, BIBO stood out due to its large SHG response (3.2 pm/V, about $8.2 \times KDP$), relatively large birefringence (0.161@1014 nm) and has inspirited a series of compounds with large SHG response like $BaBiBO_4$ [28], $Bi_2O_2CO_3$ [29] and $MBi_2B_2O_7(M=Ca,Sr)$ [30] etc. According to first-principles investigation, the large SHG of BIBO mainly derived from the (BiO_4)⁵⁻ anionic group [31]. Recently the

 SbB_3O_6 (SBBO) [32], isostructural with BIBO, was synthesized. It shows a weaker SHG (about 3.5 \times KDP), but stronger birefringence (0.291@546 nm, 0.256@1014 nm) than BIBO (0.161@1014 nm), which confused us and stimulated us to find out the origination of this difference.

All the above differences constitute the main aim and content of present paper. The electronic structures and optical properties of AB_3O_6 (A = Bi, Sb) are investigated using the first-principles method at crystal and molecular level. According to the real-space atom-cutting method, the optical properties mainly come from the BiO/SbO and BO groups due to their strong covalent bond and optical anisotropy. The states nearby the Fermi level play an important role in determining the different response about birefringence and SHG of SBBO and BIBO.

2. Calculation details

The AB₃O₆ (A = Bi, Sb) were examined using DFT implemented in the CASTEP package [33,34]. The calculations were performed using the structures obtained from ICSD database (BIBO: ICSD-48025; SBBO [32]). The exchange–correlation functionals were evaluated within GGA-PBE [35,36], the electrons Bi (6s²6p³), Sb (5s²5p³), B(2s²2p¹) and O(2s²2p⁴) were considered as valence state. The cut-off energy of 830 eV was used, and the numerical integration of the Brillouin zone was performed using $6 \times 6 \times 4$ both for BIBO and SBBO Monkhorst – Pack k-

E-mail addresses: qunjing@xju.edu.cn (Q. Jing), mqlong@csu.edu.cn (M. Long).

^{*} Corresponding authors.

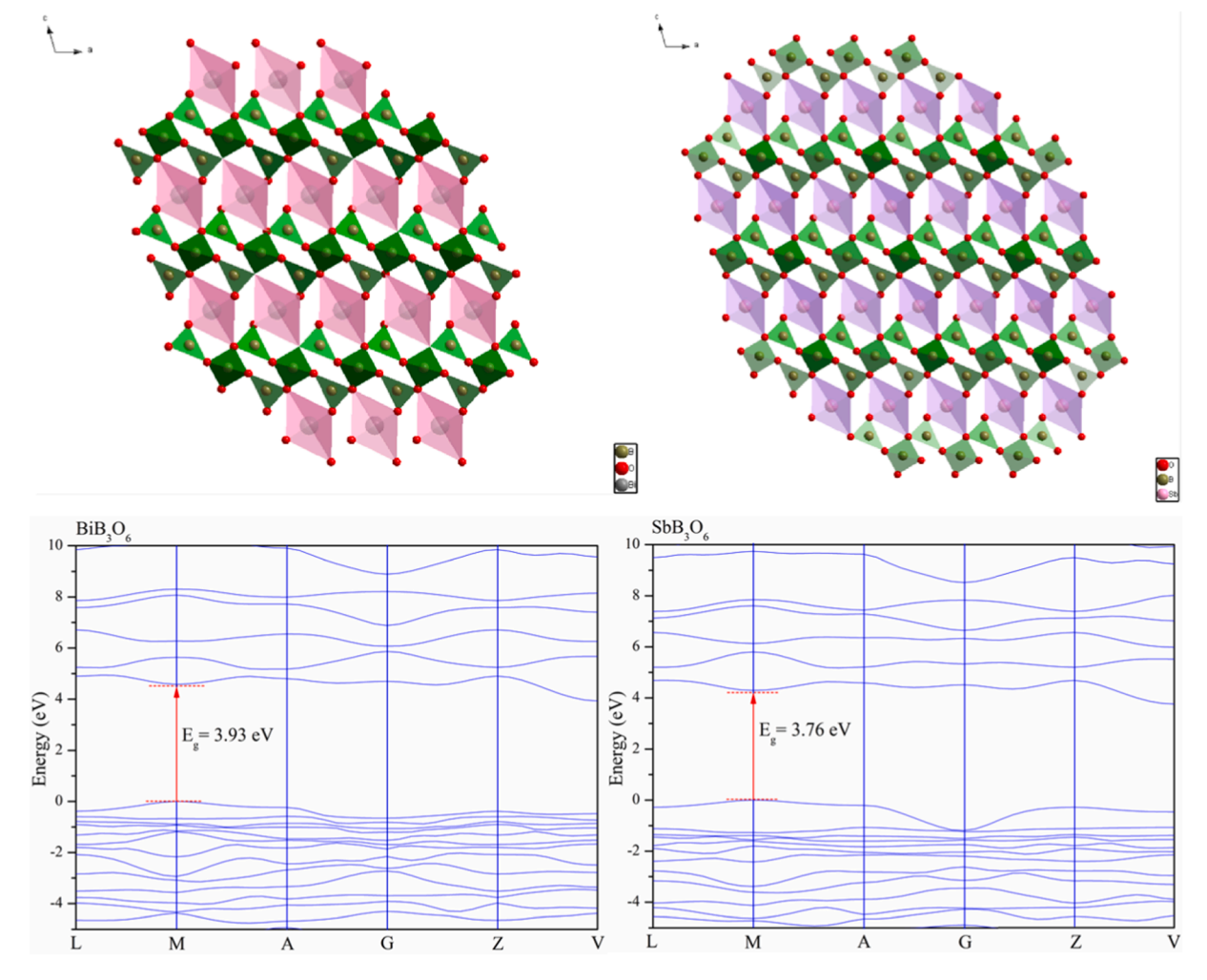


Fig. 1. The crystal structures and band structures of AB_3O_6 (A = Bi, Sb).

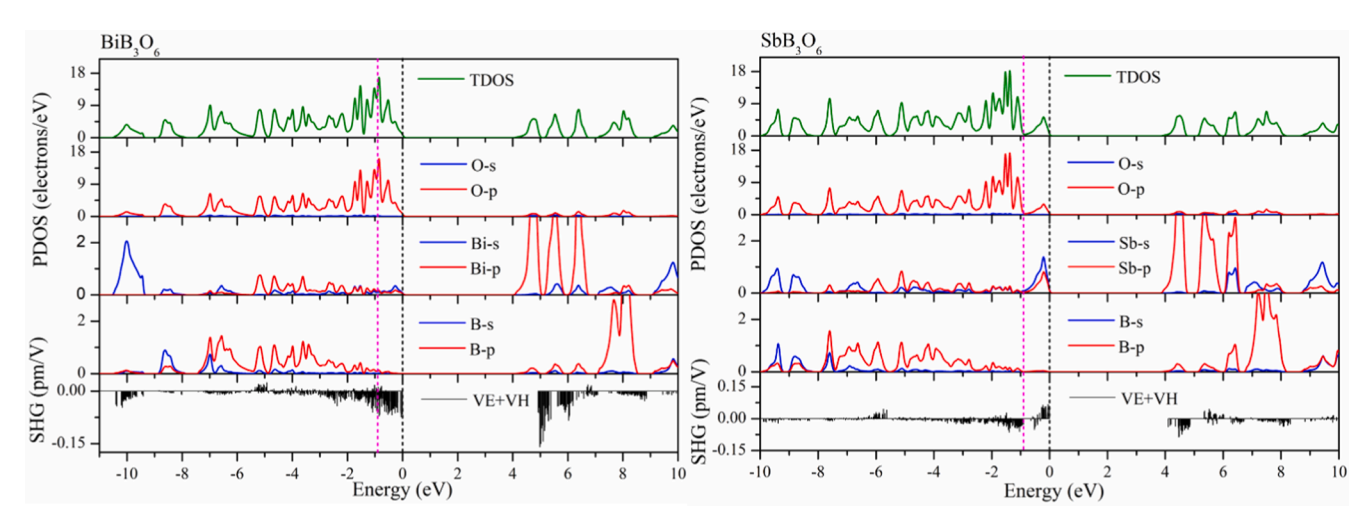


Fig. 2. The projected densities of states (PDOSs) and band resolve of AB_3O_6 (A = Bi, Sb).

point sampling. The refractive indices and birefringence were obtained using the program OptaDOS [37,38].

3. Results and discussion

3.1. The electronic structures of AB_3O_6 (A = Bi, Sb)

The crystal structures (BIBO: ICSD-48025; SBBO 32) and band structures of BIBO and SBBO are shown in Fig. 1, which exhibit a 3D

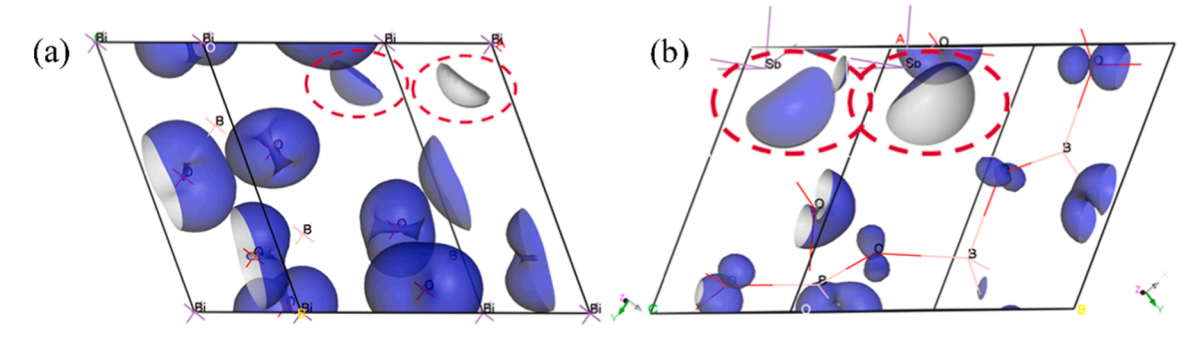


Fig. 3. Distributions of lone pair electrons around Bi (a) and Sb (b), the isosurface is set as 0.05.

Table 1 The refractive indices and birefringence values of AB_3O_6 (A = Bi, Sb).

		n _x	n_y	n_z	Δn@1014 nm	exp@1014 nm
BIBO	origin	1.918	1.775	1.747	0.171	0.161
	ВО	1.589	1.459	1.456	0.133	
	BiO	1.705	1.636	1.604	0.101	
SBBO	origin	1.947	1.793	1.691	0.256	
	ВО	1.692	1.527	1.506	0.186	
	SbO	1.729	1.657	1.545	0.184	

framework composed of BO_3 triangle, BO_4 tetrahedron and BiO_4/SbO_4 tetrahedron, BO_3 triangle and BO_4 tetrahedron are further connected to form a layer by sharing O atoms. BiO_4/SbO_4 tetrahedron acts as a bridge to connect layers to form a 3D framework. And the BIBO and SBBO are both the direct band gap semiconductor of 3.93 and 3.76 eV respectively, which is 0.41 and 0.19 eV smaller than the experimental values (4.34 and 3.95 eV severally [25,32]). Taking into account the discontinuity of the exchange correlation functional, the calculated values are in good agreement with the experimental values [39,40].

Total density of states (TDOS) and projected density of states (PDOS) are also calculated to comprehend the chemical bonding and plotted in Fig. 2. Within the range of $-10\sim$ -0.9 eV, there are obvious overlaps between B and O atom, which is B-O covalent bond. In addition, in the range of $-0.9\sim0$ eV, Bi/Sb mixing of s, p orbitals also hybridize with O 2p orbital, leading to form the stereochemically active lone pair electrons according to the lone pair electrons model [41]. Carefully observing the states lying in the region near the Fermi level (from -0.9 eV to Fermi level), it is sufficient to draw attention that more states the Sb held than Bi atoms, which might evince the greater contributions it can endow. At the bottom of the conduction band, the B-2p, O-2p and Bi/Sb-sp states also do main contribution.

To advance with a step in verifying the lone pair electrons around the Bi and Sb, the orbitals near the Fermi level are dissected. As descripted in Fig. 3, there are unquestionable asymmetric distribution around Bi and Sb, one thought leader in the positive aspects that the lone pair electron effect of Sb is overwhelming stronger than Bi.

Table 3 Bond population of AB_3O_6 (A = Bi, Sb)

BIBO bond	population	SBBO bond	population
B1-O3	0.81	B1-O3	0.87
B1-O1	0.88	B1-O1	0.67
B1-O2	0.67	B1-O2	0.8
B2-O1	0.64	B2-O1	0.57
B2-O2	0.59	B2-O3	0.65
Bi-O3	0.23	Sb-O2	0.24
Bi-O2	0.07	Sb-O1	0.07

3.2. Refractive indices and Born effective charges

As described above, AB_3O_6 (A = Bi, Sb) is expected to show the potential to exhibit excellent optical performance. Refractive indices are adequate by the program OptaDOS and listed in Table 1. The results evince that the birefringence of BIBO is 0.171@1014 nm (experimental value was 0.161@1014 nm [25]) and the birefringence of SBBO is 0.290@546 nm and 0.256@1014 nm, which is consistent with the experimental value 0.291@546 nm [32].

A real-space atom-cutting (RSAC) method can be used to intuitively exhibit contribution of each anionic group and the source of the excellent birefringence. Following the rule of cutting radii are approximately half of the covalent bond and the ionic bond, the cutting radii of Bi, Sb, B, and O are set to be 1.5, 1.2, 0.8 and 1.1 Å, respectively. Table 1 show that the main contribution to the birefringence is derived from the BiO/SbO and BO groups. From the birefringence of the decomposed groups, SbO exhibits a superior birefringence (0.184@1014 nm) much larger than BiO (0.101@1014 nm). Noting that BO group exhibits remarkable birefringence. It can be seen from Table 1 that in SBBO, the birefringence of BO group is comparable to that of SbO group, while in BIBO the birefringence of BO even exceeds the contribution of BiO.

To track down the origin of the birefringence, the Born effect charge is used to analyze individual ionic response to the external polarize light [42–44]. Δq is defined as the difference between the maximum value q_z and the minimum value q_y . Cations have a positive effect on optical response on the whole of Table 2, however there also exist differences in their actions. For BIBO, The values of Δq tend to such a trend B_1 (1.10534) > Bi (0.76350) > B₂ (0.54414), however unlike the BIBO, the

Table 2 Born effective charge q, and the difference between z and y direction ($\Delta q = |q_z| - |q_v|$)

			BIBO			SBBO			
		$\mathbf{q}_{\mathbf{x}}$	$\mathbf{q}_{\mathbf{y}}$	$\mathbf{q}_{\mathbf{z}}$	Δq	$\mathbf{q}_{\mathbf{x}}$	$\mathbf{q}_{\mathbf{y}}$	$\mathbf{q}_{\mathbf{z}}$	Δq
В	1	1.90887	1.79055	2.89589	1.10534	2.27631	1.88061	2.83915	0.95854
В	2	2.72634	2.58303	3.12717	0.54414	2.71250	2.50263	3.07660	0.57397
O	1	-1.62252	1.22245	2.27141	1.04896	1.88869	1.53491	2.57745	1.04254
O	2	-1.79556	1.67325	2.45431	0.78106	-1.84210	1.76833	1.69612	0.07221
O	3	-1.85686	1.85686	-1.80040	-0.07086	1.66433	1.22999	2.23156	1.00157
Bi/Sb	1	4.00580	3.36978	4.13328	0.76350	3.52511	2.8026	4.25535	1.45275

Table 4 The calculated SHG tensors of AB_3O_6 (A = Bi, Sb)

		d ₁₆	d ₁₄	$\mathbf{d_{22}}$	d_{23}	d _{eff} (pm/V)	Exp(pm/V)
BIBO	origin	-4.057	-2.006	-3.341	-1.343	3.6(10.9 × KDP)	3.2(8.2 × KDP)
	ВО	-1.366	0.797	-0.875	0.421		
	BiO	-2.947	-2.216	-3.217	-1.523		
SBBO	origin	-1.92	-0.481	-0.765	0.232	$1.3(3.9 \times KDP)$	$3.5 \times KDP$
	ВО	-1.396	0.643	-1.426	0.087		
	SbO	-0.904	-0.885	-0.552	0.232		

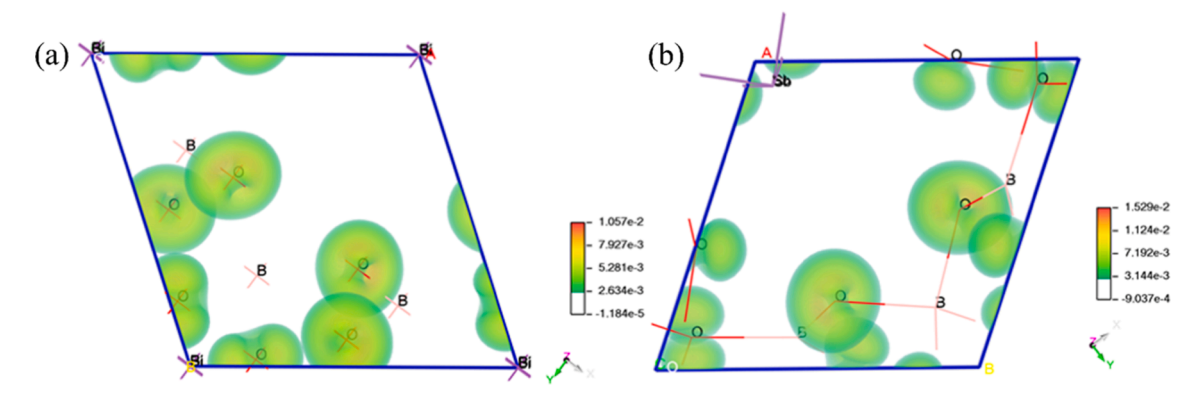


Fig. 4. The SHG densities of the VE processes for AB_3O_6 (A = Bi, Sb).

 Δq of Sb (1.45275) surpass that of maximum $B_1(0.95854)$. Furthermore the bond population of compounds are also obtained and shown in Table 3. It is observed from Table 3 that BO groups have very strong covalent bonds, as high as 0.88, much stronger than that of Bi-O(0.23)/Sb-O(0.24). In a word, two conclusions can be drawn from the above discussion, (1), the optical anisotropy of Sb is more desirable than that of Bi. (2), the large birefringence of the BO groups is derived from the large optical anisotropy and strong covalent bond of B-O.

3.3. SHG response

The SHG tensors and effective SHG coefficients of the AB_3O_6 (A = Bi, Sb) are also obtained. Taking over the largest tensor components (d_{16}) of BIBO and SBBO are 4.06 pm/V ($10.4 \times \text{KDP}$) and 1.92 pm/V ($4.9 \times \text{KDP}$) at Table 4, the effective SHG coefficients, evaluated by Kurtz and Cyvin furthermore revised by Cheng et al. [45–47], are calculated to be 3.6 pm/V ($10.9 \times \text{KDP}$) and 1.3 pm/V ($3.9 \times \text{KDP}$) respectively, which fit well with the experiment values 3.2 pm/V ($8.2 \times \text{KDP}$) and 3.5 $\times \text{KDP}$. The contribution from FBUs to SHG response are also calculated using the RSAC method. As shown in Table 4, the contribution to SHG

response mainly comes from cation centered polyhedra and anionic groups. Interestingly, the contribution of BiO groups is much greater than that of SbO groups.

Subsequently, SHG density method and band-resolved SHG response analysis are selected to exhibit each group's contribution intuitively. It has been noticed that the contribution of SHG response can be divided into two processes: Virtual-Electron (VE) and Virtual-Hole (VH), and the contribution of VH is almost negligible [48], so the SHG densities of the VE processes are displayed in Fig. 4, which contribution accounts for 74% and 78% of the total SHG response. It is demonstrated in Fig. 4 that BiO/SbO and BO groups serve as the cornerstone of the total SHG response. Recalling Fig. 2, PDOS and band resolve are discussed together in the range of $-0.9 \sim 0$ eV, the obvious negative contribution of SBBO can be clearly seen by comparing the band resolve of the two compounds, while Bi is a positive contribution, which evidences the source of SHG response with smaller SBBO.

In addition to the above methods, we further explored the optical properties of SbO and BiO groups from the molecular point of view, and calculated the frontier orbitals (shown in Fig. 5), the polarizability and hyperpolarizability of SbO and BiO groups by using def2-tzvpdz basis set

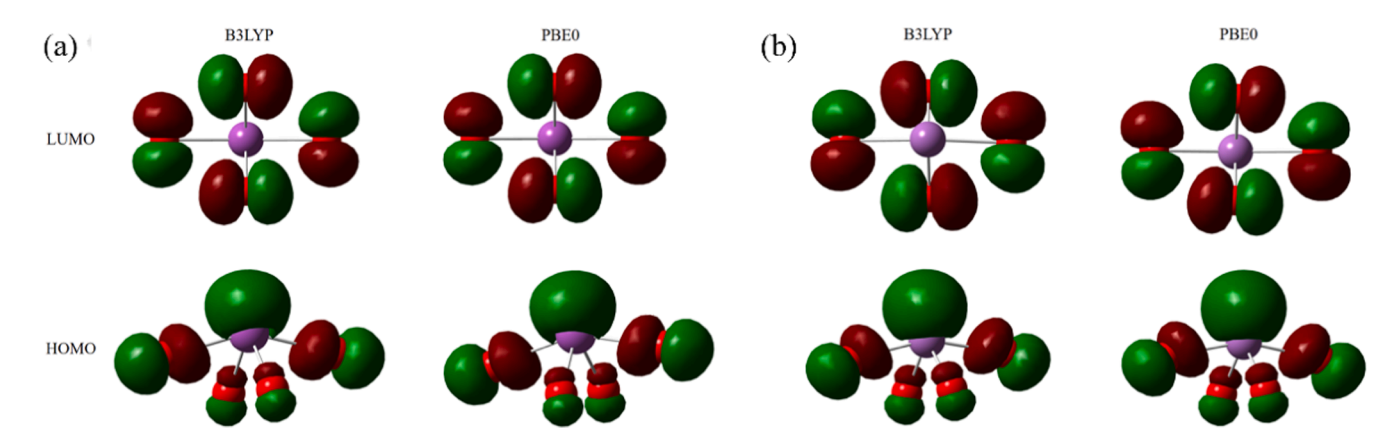


Fig. 5. The frontier molecular orbitals of BiO(a) and SbO(b) groups, purple for cations and red for oxygen atoms. (For interpretation of the references to colour in this figure legend, the reader is referred to the web version of this article.)

Table 5 Calculated properties of SbO and BiO (polarizability anisotropy (α), first hyperpolarizability tensor (β), and HOMO – LUMO Gap (Eg))

		B3LYP	PBE0	Δn/deff
SbO ₄	α	431	381	0.184
	β	7.07	5.79	1.00
	E_{g}	0.96	1.23	
BiO_4	α	388	351	0.101
	β	-38.5	-10.8	3.51
	$\mathbf{E}_{\mathbf{g}}$	0.76	1.02	

under B3LYP and PBE0 functional with Gaussian 09 software package [49].

As shown in Fig. 5, the nonbond 2p orbital of O occupies the lowest unoccupied molecular orbital (LUMO). In the highest occupied molecular orbital (HOMO), there are mainly Sb/Bi-s and O-p orbitals. Both groups show significant optical anisotropy.

Table 5 gives the polarizability and hyperpolarizability of SbO and BiO groups. As shown in Table 5, the polarizability of SbO group is larger than BiO group, which is in line with the trend of birefringence. While the hyperpolarizability of SbO groups is smaller than BiO groups, and the hyperpolarizability of anionic groups own similar tendency like SHG response of BIBO and SBBO. That's to say the BiO group can improve the SHG response of the material. The calculated optical properties show that the HOMO-LUMO gaps of the two groups are close to each other.

4. Conclusions

In a word, the electronic structures, refractive indices and birefringence of AB₃O₆ (A = Bi, Sb) are calculated using the first-principles method. The obtained results are in good agreement with experimental values. The different response about birefringence and SHG are further investigated using Born effective charges, real-space atom-cutting method, and the molecular orbitals and molecular optical properties. The results show that the anionic groups and cation-centered polyhedron exhibits excellent optical properties due to their strong covalent bond and optical anisotropy. At molecular level, the SbO groups own stronger polarizability anisotropy (a) and smaller first hyperpolarizability tensor (β) comparison with BiO groups. As for these crystals, the states nearby the Fermi level of SBBO give positive and negative contribution to birefringence, and SHG, respectively, which make it own stronger birefringence and smaller SHG comparison with BIBO. One can instructive us to design and synthesize new NLO materials with excellent optical properties.

CRediT authorship contribution statement

Xuerui Shi: Formal analysis, Data curation, Writing – original draft. Qun Jing: Supervision, Project administration, Writing – review & editing. Ming-Hsien Lee: Software. Haibin Cao: Software. Mengqiu Long: Writing – review & editing.

Declaration of Competing Interest

The authors declare that they have no known competing financial interests or personal relationships that could have appeared to influence the work reported in this paper.

Acknowledgments

This work was supported by the Natural Science Foundation of Xinjiang Uygur Autonomous Region of China (Grant No. 2018D01C072).

References

- [1] D.F. Eaton, Nonlinear optical materials, Sci 253 (5017) (1991) 281-287.
- [2] D.A. Kleinman, Theory of Second Harmonic Generation of Light, Phys. Rev. 128 (4) (1962) 1761–1775.
- [3] N. Ye, C. Tu, X. Long, M. Hong, Recent Advances in Crystal Growth in China: Laser, Nonlinear Optical, and Ferroelectric Crystals, Cryst. Growth Des. 10 (11) (2010) 4672–4681.
- [4] Y. Pan, Influence of N-vacancy on the electronic and optical properties of bulk GaN from first-principles investigations, Int J Energ Res 45 (10) (2021) 15512–15520.
- [5] Y. Pan, E. Yu, First-principles investigation of electronic and optical properties of H-doped FeS₂, Int. J. Energ. Res. 45 (7) (2021) 11284–11293.
- [6] Y. Pan, J. Zhang, Influence of noble metals on the electronic and optical properties of the monoclinic ZrO₂: A first-principles study, Vacuum 187 (2021) 110112, https://doi.org/10.1016/j.vacuum.2021.110112.
- [7] Y. Pan, The influence of Ag and Cu on the electronic and optical properties of ZrO from first-principles calculations, Mater. Sci. Semicond. Process. 135 (2021) 106084. https://doi.org/10.1016/j.mssp.2021.106084.
- [8] Y. Pan, The influence of N-vacancy on the electronic and optical properties of bulk InN nitrides, Mat. Sci. Eng. B 271 (2021) 115265, https://doi.org/10.1016/j. mseb.2021.115265.
- [9] H. Wu, H. Yu, Z. Yang, X. Hou, X. Su, S. Pan, K.R. Poeppelmeier, J.M. Rondinelli, Designing a Deep-ultraviolet Nonlinear Optical Material with a Large Second Harmonic Generation Response, J. Am. Chem. Soc. 135 (11) (2013) 4215–4218.
- [10] H. Wu, S. Pan, K.R. Poeppelmeier, H. Li, D. Jia, Z. Chen, X. Fan, Y. Yang, J. M. Rondinelli, H. Luo, K₃B₆O₁₀Cl: a New Structure Analogous to Perovskite with a Large Second Harmonic Generation Response and Deep UV Absorption Edge, J. Am. Chem. Soc. 133 (20) (2011) 7786–7790.
- [11] G. Shi, Y. Wang, F. Zhang, B. Zhang, Z. Yang, X. Hou, S. Pan, K.R. Poeppelmeier, Finding the Next Deep-Ultraviolet Nonlinear Optical Material: NH₄B₄O₆F, J. Am. Chem. Soc. 139 (31) (2017) 10645–10648.
- [12] B. Zhang, G. Shi, Z. Yang, F. Zhang, S. Pan, Fluorooxoborates: Beryllium-Free Deep-Ultraviolet Nonlinear Optical Materials without Layered Growth, Angew. Chem. Int. Ed. Engl. 56 (14) (2017) 3916–3919.
- [13] X. Wang, Y. Wang, B. Zhang, F. Zhang, Z. Yang, S. Pan, CsB₄O₆F: A Congruent-Melting Deep-Ultraviolet Nonlinear Optical Material by Combining Superior Functional Units, Angew. Chem. Int. Ed. Engl. 56 (45) (2017) 14119–14123.
- [14] M. Mutailipu, M. Zhang, B. Zhang, L. Wang, Z. Yang, X. Zhou, S. Pan, SrB₅O₇F₃ Functionalized with [B₅O₉F₃]⁶ Chromophores: Accelerating the Rational Design of Deep-Ultraviolet Nonlinear Optical Materials, Angew. Chem. Int. Ed. Engl. 57 (21) (2018) 6095–6099.
- [15] Y. Wang, B. Zhang, Z. Yang, S. Pan, Cation-Tuned Synthesis of Fluorooxoborates: Towards Optimal Deep-Ultraviolet Nonlinear Optical Materials, Angew. Chem. Int. Ed. Engl. 57 (8) (2018) 2150–2154.
- [16] M. Mutailipu, K.R. Poeppelmeier, S. Pan, Borates: A Rich Source for Optical Materials, Chem. Rev. 121 (3) (2021) 1130–1202.
- [17] Z. Zhang, Y. Wang, B. Zhang, Z. Yang, S. Pan, Polar Fluorooxoborate, NaB₄O₆F: A Promising Material for Ionic Conduction and Nonlinear Optics, Angew. Chem. Int. Ed. Engl. 57 (22) (2018) 6577–6581.
- [18] C. Chen, Y. Wu, A. Jiang, B. Wu, G. You, R. Li, S. Lin, New nonlinear-optical crystal: LiB₃O₅, J. Opt. Soc. Am. B 6 (4) (1989).
- [19] Y. Wu, T. Sasaki, S. Nakai, A. Yokotani, H. Tang, C. Chen, CsB₃O₅: A new nonlinear optical crystal, Appl. Phys. Lett. 62 (21) (1993) 2614–2615.
- [20] C.T. Chen, G.L. Wang, X.Y. Wang, Z.Y. Xu, Deep-UV nonlinear optical crystal KBe₂BO₃F₂-discovery, growth, optical properties and applications, Appl. Phys. B-Lasers O 97 (1) (2009) 9–25.
- [21] C. Chen, Z. Xu, D. Deng, J. Zhang, G.K.L. Wong, B. Wu, N. Ye, D. Tang, The vacuum ultraviolet phase-matching characteristics of nonlinear optical KBe₂BO₃F₂ crystal, Appl. Phys. Lett. 68 (21) (1996) 2930–2932.
- [22] K.M. Ok, Functional layered materials with heavy metal lone pair cations, Pb²⁺, Bi³

 +, and Te⁴⁺, Chem. Commun. (Camb.) 55 (85) (2019) 12737–12748.
- [23] A. Walsh, G.W. Watson, Influence of the anion on lone pair formation in Sn(II) monochalcogenides: A DFT study, J. Phys. Chem. B 109 (40) (2005) 18868–18875.
- [24] H. Hellwig, J. Liebertz, L. Bohaty, Exceptional large nonlinear optical coefficients in the monoclinic bismuth borate BiB₃O₆ (BIBO), Solid State Commun. 109 (4) (1999) 249–251.
- [25] H. Hellwig, J. Liebertz, L. Bohatý, Linear Optical Properties of the Monoclinic Bismuth Borate BiB₃O₆, J. Appl. Phys. 88 (1) (2000) 240–244.
- [26] X. Dong, L. Huang, C. Hu, H. Zeng, Z. Lin, X. Wang, K.M. Ok, G. Zou, CsSbF2SO4: An Excellent Ultraviolet Nonlinear Optical Sulfate with a KTiOPO4 (KTP)-type Structure, Angew. Chem. Int. Ed. Engl. 58 (20) (2019) 6528–6534.
- [27] M. Luo, F. Liang, Y. Song, D. Zhao, N. Ye, Z. Lin, Rational Design of the First Lead/ Tin Fluorooxoborates MB₂O₃F₂ (M = Pb, Sn), Containing Flexible Two-Dimensional B₆O₁₂F₆ (infinity) Single Layers with Widely Divergent Second Harmonic Generation Effects, J. Am. Chem. Soc. 140 (22) (2018) 6814–6817.
- [28] J. Barbier, N. Penin, A. Denoyer, L.M.D. Cranswick, BaBiBO₄, a novel non-centrosymmetric borate oxide, Solid State Sci. 7 (9) (2005) 1055–1061.
- [29] A.H. Reshak, S. Auluck, Dispersion of the linear and nonlinear optical susceptibilities of Bismuth subcarbonate Bi₂O₂CO₃: DFT calculations, Opt. Mater. 38 (2014) 80–86.
- [30] J. Barbier, L.M.D. Cranswick, The non-centrosymmetric borate oxides, MBi₂B₂O₇ (M=Ca, Sr), J. Solid State Chem. 179 (12) (2006) 3958–3964.
- [31] Z. Lin, Z. Wang, C. Chen, M.-H. Lee, Mechanism for linear and nonlinear optical effects in monoclinic bismuth borate (BiB₃O₆) crystal, J. Appl. Phys. 90 (11) (2001) 5585–5590.

- [32] Y. Liu, X. Liu, S. Liu, Q. Ding, Y. Li, L. Li, S. Zhao, Z. Lin, J. Luo, M. Hong, An Unprecedented Antimony(III) Borate with Strong Linear and Nonlinear Optical Responses, Angew. Chem. Int. Ed. Engl. 59 (20) (2020) 7793–7796.
- [33] S.J. Clark, M.D. Segall, C.J. Pickard, P.J. Hasnip, M.L.J. Probert, K. Refson, M. C. Payne, First principles methods using CASTEP, Z Kristallogr 220 (5/6) (2005).
- [34] M.D. Segall, P.J.D. Lindan, M.J. Probert, C.J. Pickard, P.J. Hasnip, S.J. Clark, M. C. Payne, First-principles simulation: ideas, illustrations and the CASTEP code, J. Phys.: Condens. Matter 14 (11) (2002) 2717–2744.
- [35] J.P. Perdew, K. Burke, M. Ernzerhof, Generalized Gradient Approximation Made Simple, Phys. Rev. Lett. 77 (18) (1996) 3865–3868.
- [36] M. Ernzerhof, G.E. Scuseria, Assessment of the Perdew–Burke–Ernzerhof exchange-correlation functional, J. Chem. Phys. 110 (11) (1999) 5029–5036.
- [37] R.J. Nicholls, A.J. Morris, C.J. Pickard, J.R. Yates, OptaDOS a new tool for EELS calculations, J. Phys.: Conf. Ser. (2012) 371.
- [38] A.J. Morris, R.J. Nicholls, C.J. Pickard, J.R. Yates, OptaDOS: A Tool for Obtaining Density of States, Core-level and Optical Spectra from Electronic Structure Codes, Comput. Phys. Commun. 185 (5) (2014) 1477–1485.
- [39] H. Xiao, J. Tahir-Kheli, W.A. Goddard, Accurate Band Gaps for Semiconductors from Density Functional Theory, J. Phys. Chem. Lett. 2 (3) (2011) 212–217.
- [40] M.K. Chan, G. Ceder, Efficient Band Gap Prediction for Solids, Phys. Rev. Lett. 105 (19) (2010), 196403.
- [41] A. Walsh, D.J. Payne, R.G. Egdell, G.W. Watson, Stereochemistry of Post-transition Metal Oxides: Revision of the Classical Lone Pair Model, Chem. Soc. Rev. 40 (9) (2011) 4455–4463.
- [42] N.A. Spaldin, A beginner's guide to the modern theory of polarization, J. Solid State Chem. 195 (2012) 2–10.
- [43] Q. Jing, G. Yang, J. Hou, M. Sun, H. Cao, Positive and negative contribution to birefringence in a family of carbonates: A Born effective charges analysis, J. Solid State Chem. 244 (2016) 69–74.

- [44] R. Resta, D. Vanderbilt, Theory of polarization: A modern approach. 105 (2007)
- [45] S.K. Kurtz, T.T. Perry, A Powder Technique for the Evaluation of Nonlinear Optical Materials, J. Appl. Phys. 39 (8) (1968) 3798–3813.
- [46] S.J. Cyvin, J.E. Rauch, J.C. Decius, Theory of Hyper-Raman Effects (Nonlinear Inelastic Light Scattering): Selection Rules and Depolarization Ratios for the Second-Order Polarizability, J. Chem. Phys. 43 (11) (1965) 4083–4095.
- [47] X. Cheng, M.-H. Whangbo, G.-C. Guo, M. Hong, S. Deng, The Large Second-Harmonic Generation of LiCs₂PO₄ is caused by the Metal-Cation-Centered Groups, Angew. Chem. Int. Ed. Engl. 57 (15) (2018) 3933–3937.
- [48] B.B. Zhang, M.H. Lee, Z.H. Yang, Q. Jing, S.L. Pan, M. Zhang, H.P. Wu, X. Su, C. S. Li, Simulated pressure-induced blue-shift of phase-matching region and nonlinear optical mechanism for K₃B₆O₁₀X (X = Cl, Br), Appl. Phys. Lett. 106 (3) (2015).
- [49] Frisch M. J., Trucks G. W., Schlegel H. B., Scuseria G. E., Robb M. A., Cheeseman J. R., Scalmani G., Barone V., Petersson G. A., Nakatsuji H., Li X., Caricato M., Marenich A. V., Bloino J., Janesko B. G., Gomperts R., Mennucci B., Hratchian H. P., Ortiz J. V., Izmaylov A. F., Sonnenberg J. L., Williams F., Ding F., Lipparini F., Egidi F., Goings J., Peng B., Petrone A., Henderson T., Ranasinghe D., Zakrzewski V. G., Gao J., Rega N., Zheng G., Liang W., Hada M., Ehara M., Toyota K., Fukuda R., Hasegawa J., Ishida M., Nakajima T., Honda Y., Kitao O., Nakai H., Vreven T., Throssell K., Montgomery Jr J. A., Peralta J. E., Ogliaro F., Bearpark M. J., Heyd J. J., Brothers E. N., Kudin K. N., Staroverov V. N., Keith T. A., Kobayashi R., Normand J., Raghavachari K., Rendell A. P., Burant J. C., Iyengar S. S., Tomasi J., Cossi M., Millam J. M., Klene M., Adamo C., Cammi R., Ochterski J. W., Martin R. L., Morokuma K., Farkas O., Foresman J. B., Fox D. J. Gaussian 09, Revision E.01. 2013., Wallingford, CT.